Lithuanian Journal of Physics
Vol. **63**, No. 3, pp. 148–154 (2023)
ISSN 1648-8504 eISSN 2424-3647
DOI: https://doi.org/10.3952/physics.2023.63.3.5

SUM-FREQUENCY GENERATION AND AMPLIFICATION PROCESSES IN SEMICONDUCTOR SUPERLATTICES

V. Čižas [a], N. Alexeeva [a], K. Alekseev [a], and G. Valušis [a, b]

[a] *Department of Optoelectronics, Center for Physical Sciences and Technology, Saulėtekio 3, 10257 Vilnius, Lithuania*
[b] *Photonics and Nanotechnology Institute, Faculty of Physics, Vilnius University, Saulėtekio 3, 10257 Vilnius, Lithuania*
Email: vladislovas.cizas@ftmc.lt

Received 27 September 2023; accepted 28 September 2023

Semiconductor superlattices are very well-known structures due to their specific electron transport properties, making them extremely attractive to be employed in electronic or optoelectronic devices. The interest in such structures has been recently additionally stirred up due to the first successful experimental demonstration of parametric gain in GaAs/AlGaAs superlattices, resulting in the generation of harmonics, half-harmonics and fractional harmonics. This invention paves the way for a successful realization of superlattice-based generators and amplifiers up to the terahertz frequency range. Despite the emerging experimental results and decade-long theoretical research, unresolved aspects, related to the physical processes inside the superlattices, persist. Lately, the biasing effect was extensively analysed for the case of degenerate processes in the superlattice; however, the non-degenerate case was left out of frame until now. Within this research, we further expand the boundaries of previous investigation by exploring the differences of non-degenerate processes. The study uncovers the asymmetry appearance of the probe field vs. relative phase dependences as well as the possibility of parametric fractional frequency generation. Finally, the concept of energy reflow between two participating probes is predicted and discussed.

Keywords: superlattice, non-degenerate process, parametric gain, Bloch gain

1. Introduction

Semiconductor superlattices, best known for their ability to mimic crystal lattice with unnaturally large lattice constants, are prominent quantum structures exploited across a wide range of terahertz (THz) frequency range-based applications [1]. Unique electronic transport properties reveal a diverse variety of physical effects, providing an additional flexibility for the superlattice-based generators and/or amplifiers, resulting in their employment in a broad range of modern electronic and optoelectronic devices, like quantum cascade lasers, parametric oscillators and frequency multipliers [2–5].

The exploration of high-frequency gain effect attracts exceptional attention, as according to the theoretical studies and primary experiments, enormous gain levels of high frequency (up to the THz range) are expected [6–11]. This is an eye-catching feature because of the possibility of comparably simple sub-harmonic and fractional harmonic generation [12]. The successful realization of semiconductor superlattice-based devices, due to their achievable generation powers and cost efficiency, is expected to ensure a tangible leap for the THz-based applicational solutions and further research activities [13–14].

Recently, we have demonstrated that the superlattices can be an attractive environment for the efficient parametric gain at room temperature [15]. However, despite of the successful proof-of-concept experiment realization and decade-lasting theoretical research, a lot of unresolved aspects of the processes that occur in the superlattices are still unrevealed.

In this work, we explore the non-degenerate processes (containing two probe frequencies,

participating in the gain process), occurring in a biased semiconductor superlattice. Taking into account the previously conducted experimental data, we dismiss the typically-used small signal gain model, wherein the probe fields are assumed to be negligibly small, but instead employ the large-signal gain model. By analysing the gain processes, recorded during the proof-of-concept experiment, we reveal the similarities and differences of the non-degenerate gain process compared to those of recently disclosed degenerate gain processes (one probe field employed) [16]. More specifically, it includes the asymmetry appearance in electric field vs. relative phase dependences, the possibility of the pure parametric generation of fractional frequency (not available for the degenerate process) and the accentuated transition from the pure Bloch to the parametric gain mechanism. Furthermore, the concept of energy reflow between the two-probe fields is predicted and discussed.

2. Materials and methods

A single miniband semiconductor superlattice, with the electric fields applied along the superlattice growth axis, is considered within this research. The considered superlattice is a 30-period GaAs/AlGaAs superlattice, comprising 5 nm GaAs wells and 1 nm $Al_{0.3}Ga_{0.7}As$ barriers. Doping of $N \approx 10^{16}$ cm^{-1} aligns with the Kroemer *NL* criterion requirements, preventing the domain formation. As shown during the proof-of-concept experiment [15], for the abovementioned structure, the application of the proper combination of ac and dc electric fields result in the generation of harmonics, sub-harmonics and fractional harmonics.

The total applied electric field is assumed as the combination of dc-ac pump fields and ac probe fields. Taking into account the experimental results, the probe electric fields cannot be treated as negligibly small. Hence, the small signal gain model cannot be applied, and the large signal gain model has to be employed. An explicit description of the large signal gain model is given in Ref. [16], where the degenerate processes are analyzed in details. For the case of non-degenerate mechanism, we introduce the additional probe electric field which results in

$$F_{\mathrm{tot}}(t) = F_{\mathrm{dc}} + F_{\mathrm{ac}}\cos(x) + F_1\cos\left(\frac{m_1}{n_1}x+\varphi_1\right) + F_2\cos\left(\frac{m_2}{n_2}x+\varphi_2\right), \quad (1)$$

where the electric fields are represented in the units of critical electric field $F_{\mathrm{i}} = E_{\mathrm{i}}/E_{\mathrm{cr}}$ as described in Ref. [16], F_{dc} and F_{ac} describe biasing by external ac and dc pump fields in terms of the Esaki–Tsu critical electric field, $E_{\mathrm{cr}} = \hbar/ed\tau$ is the Esaki–Tsu critical electric field, $x = \omega_0 t$, and F_1 and F_2 describe the electric field of two ac probes of frequencies $\frac{m_1}{n_1}\omega_0$ and $\frac{m_2}{n_2}\omega_0$, in terms of the Esaki–Tsu critical electric field. Such applied electric field results in the total relative power to be equal to

$$\bar{P}(\varphi_1, \varphi_2, E_1, E_2) = \bar{P}_1 + \bar{P}_2, \quad (2)$$

where

$$\overline{P_{1,2}} = \frac{F_{1,2}}{2\pi(n_1 n_2)} \times \int_0^{2\pi n_1 n_2} \frac{2F_{\mathrm{tot}}(x)\mathrm{d}x}{1+F_{\mathrm{tot}}^2(x)} \cos\left(\frac{m_{1,2}}{n_{1,2}}x+\varphi_{1,2}\right). \quad (3)$$

Here $\bar{P}_{\mathrm{i}} = P/P_0$ is the dimensionless relative power, where $P_0 = eNv_{\mathrm{p}}E_{\mathrm{cr}}$, v_p is the peak electron velocity, and E_{cr} is the Esaki–Tsu critical field. Gain on particular frequency will occur only if the corresponding relative power is negative, $\bar{P}_{\mathrm{i}} < 0$ [17]. As already shown, in case the electric field strengths of both probe fields are equal ($F_1 = F_2$), the non-degenerate process can be treated as degenerate, thus, this case was not exclusively analyzed during this research. Furthermore, we will not separate the analysed processes into down- and up-conversion ones as is done in the abovecited articles. In this study, the effect on one of the probes with the predefined second probe field is mostly analyzed, thus the difference between the down- and up-conversion processes is not expected to introduce any difference. Further analysis of the differences between up- and down-conversion processes is foreseen in succeeding publications along with the analysis of the suggested replacement for the Manley–Rowe relations, which were shown to be nonapplicable to describe gain processes in the superlattices under the Esaki–Tsu regime [15, 18].

3. Results and discussion

In the case of non-degenerate gain processes, the frequency $\frac{m_2}{n_2}\omega_0$, the electric field strength $\bar{F}_2$ and the relative phase φ_2 of the second probe electric field should be additionally taken into account. In order to decrease the number of independent variables, we have analyzed only the non-degenerate relations observed in the experiment. Specifically, these include 4/3 + 8/3 as an example of fractional harmonics gain and 1/2 + 3/2 as an example of subharmonics gain. The lower harmonics in any non-degenerate process here and beyond will be labelled as probe 1, and higher harmonics will be indicated as probe 2. Figure 1 depicts the probe 1 electric field strength vs. probe 1 relative phase for different probe 2 relative phases in the case of 4/3 + 8/3 non-degenerate process, $F_{dc} = 4$, $F_{ac} = 3$, $F_2 = 2$. The coloured areas show that under the combination of particular conditions, probe 1 will be amplified. Blank areas show that probe 1 will not be amplified under particular conditions. As one may recall, for the case of degenerate process the probe field strength vs. relative phase dependences always exhibit π-symmetry [16]. This is a sharp difference compared to the non-degenerate process. The participation of the second probe electric field can drastically change the generation/amplification profile, resulting in different possibilities to generate/amplify the probe signal. Thus, for example, in Fig. 1(a), one may note the formation of the generation area ($\varphi_1 \approx \pi$) and the formation of amplification islands ($\varphi_1 \approx 0$) – the situation unavailable for the case of degenerate process. In this case, the generation area means that the probe 1 signal can be generated starting from the small signal probe 1 electric field strength, and the amplification islands depict the conditions when the probe 1 signal is amplified, starting from the threshold-defined probe 1 electric field strength.

The differences of the degenerate and non-degenerate processes are evidently revealed in Fig. 2, depicting the dependence of the maximum relative power of probe 1 (relative phases φ_1 and φ_2 are optimized to achieve the maximal probe 1 relative power) on the biasing conditions for different probe 2 electric field strengths in the 4/3+8/3 non-degenerate process. The generation picture changes drastically. First of all, analyzing the $F_{ac} > F_{dc}$ conditions (red dots on the main graph and the upper inset) one may note that the generation of fractional harmonics becomes available, which is in a sharp contrast to the case of degenerate process, where only amplification islands are formed under specific biasing conditions. Furthermore, the abovementioned generation is probe 1 phase dependent, indicating the parametric nature of the observed generation process.

Second, the changes occurring in the $F_{dc} > F_{ac}$ area need to be analyzed. It is worth noting that in the case of degenerate processes in the $F_{dc} > F_{ac}$ area, the coexistence of two amplification mechanisms is expected: parametric gain and Bloch gain. As shown earlier, the dominating mechanism is pump ac bias dependent: when the pump ac bias is low, the phase independent Bloch gain is dominant and when the pump ac bias is high,

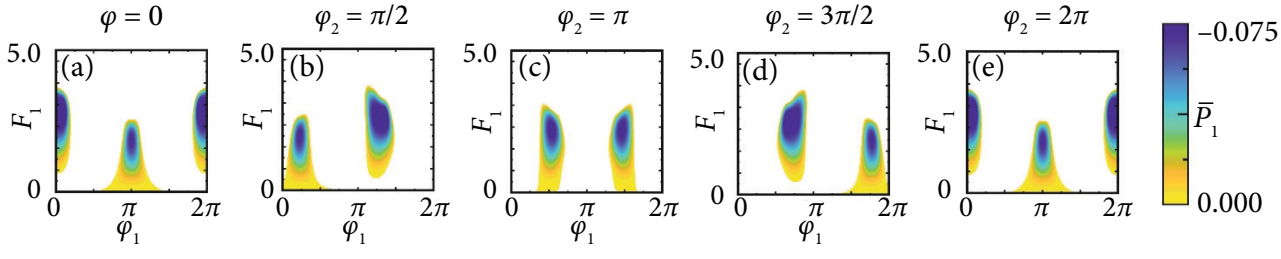

Fig. 1. Probe 1 electric field dependence vs. probe 1 relative phase for the case of different probe 2 relative phase in the 4/3+8/3 non-degenerate process. $F_{dc} = 4$, $F_{ac} = 3$, $F_2 = 2$. Coloured areas depict the conditions where the gain in the superlattice is available. Blank areas depict the conditions where the gain is absent. One may note, in contrast to the degenerate process, the assymetry of the dependences and different types of gain available for the same conditions, but the probe 1 phase. These are the amplification island (amplification from the treshold electric field strength) and generation from the small electric field strength.

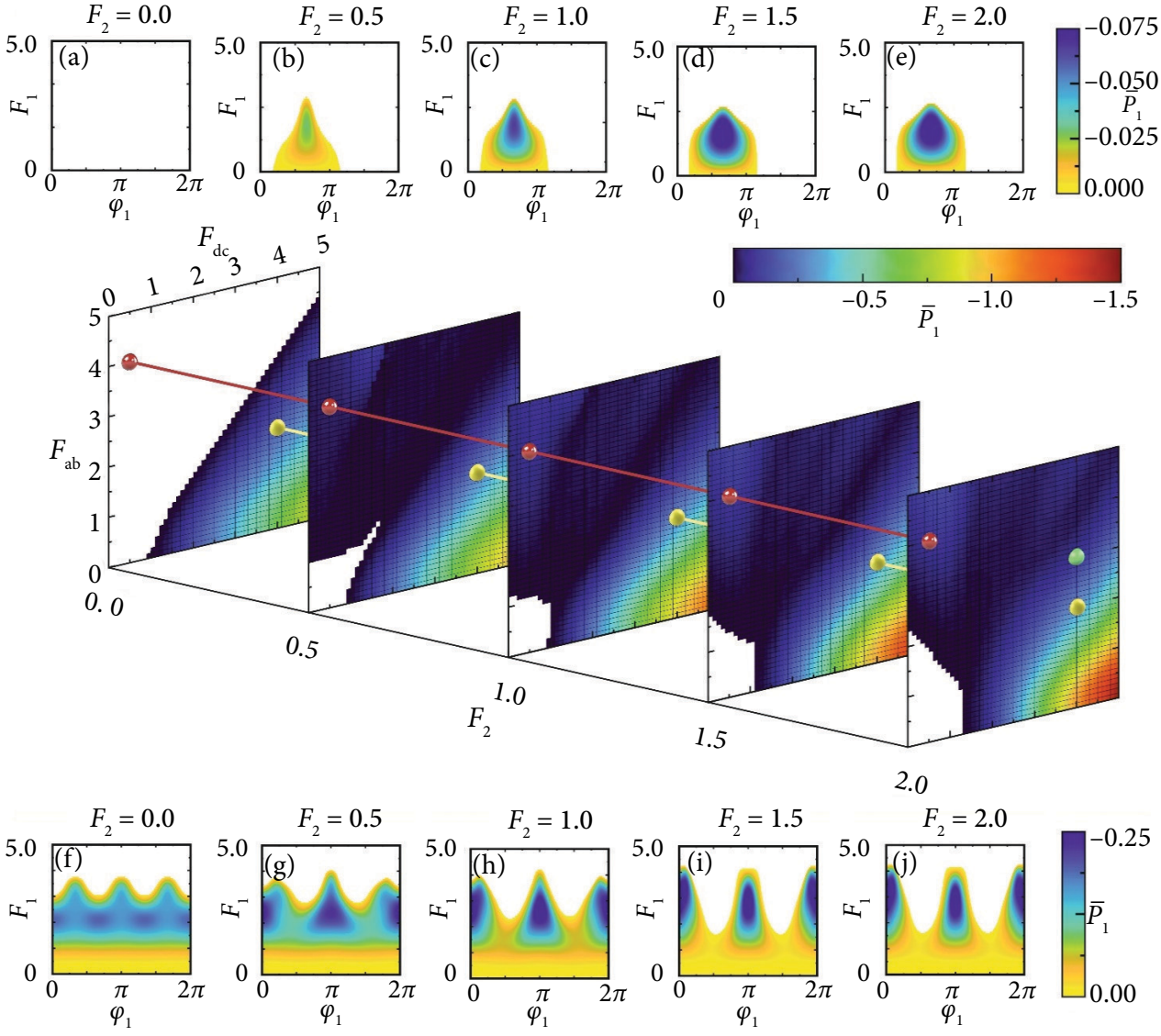

Fig. 2. Main figure: the maximal probe 1 relative power dependence on biasing conditions and probe 2 electric field strength in the case of 4/3+8/3 non-degenerate gain process. Coloured areas depict the conditions when generation is available, while blank areas depict the conditions when generation is absent. Upper insets (a–e): probe 1 electric field strength vs. probe 1 phase dependence for $F_{dc} = 0.5$, $F_{ac} = 4$ and $F_2 = 0{:}0.5{:}2$, corresponding to red dots on the main figure. Note the appearance of fractional harmonics generation in the $F_{ac} > F_{dc}$ area – the feature unavailable within the degenerate gain process. Bottom insets (f–j): probe 1 electric field strength vs. probe 1 phase dependence for $F_{dc} = 4$, $F_{ac} = 3$ and $F_2 = 0{:}0.5{:}2$, corresponding to yellow dots on the main figure. Note the increasing domination of the phase-dependent parametric gain mechanism with the increase of probe 2 electric field strength. Green dots correspond to the biasing conditions for the case, depicted in Fig. 1.

the parametric gain takes over [16]. The same conversion process remains in the case of non-degenerate gain and is even more expressed with the increase of probe 2 electric field strength (cf. the bottom inset (f–j) and yellow dots on the main graph of Fig. 2). This is disclosed in the increased relative power and even larger phase dependence.

The tendency of the increased parametric generation region remains for the case of half-harmonics (see Fig. 3(a) depicting the case of $1/2\omega_0$). Additional analysis of the total and probe 2 powers, corresponding to the maximal probe 1 power, may unveil additional interesting considerations, related to the energy exchange between two probe electric fields. One may note that upon particular pump biasing conditions, the probe 2 power may be either negative (representing emission at probe 2 frequency) or positive

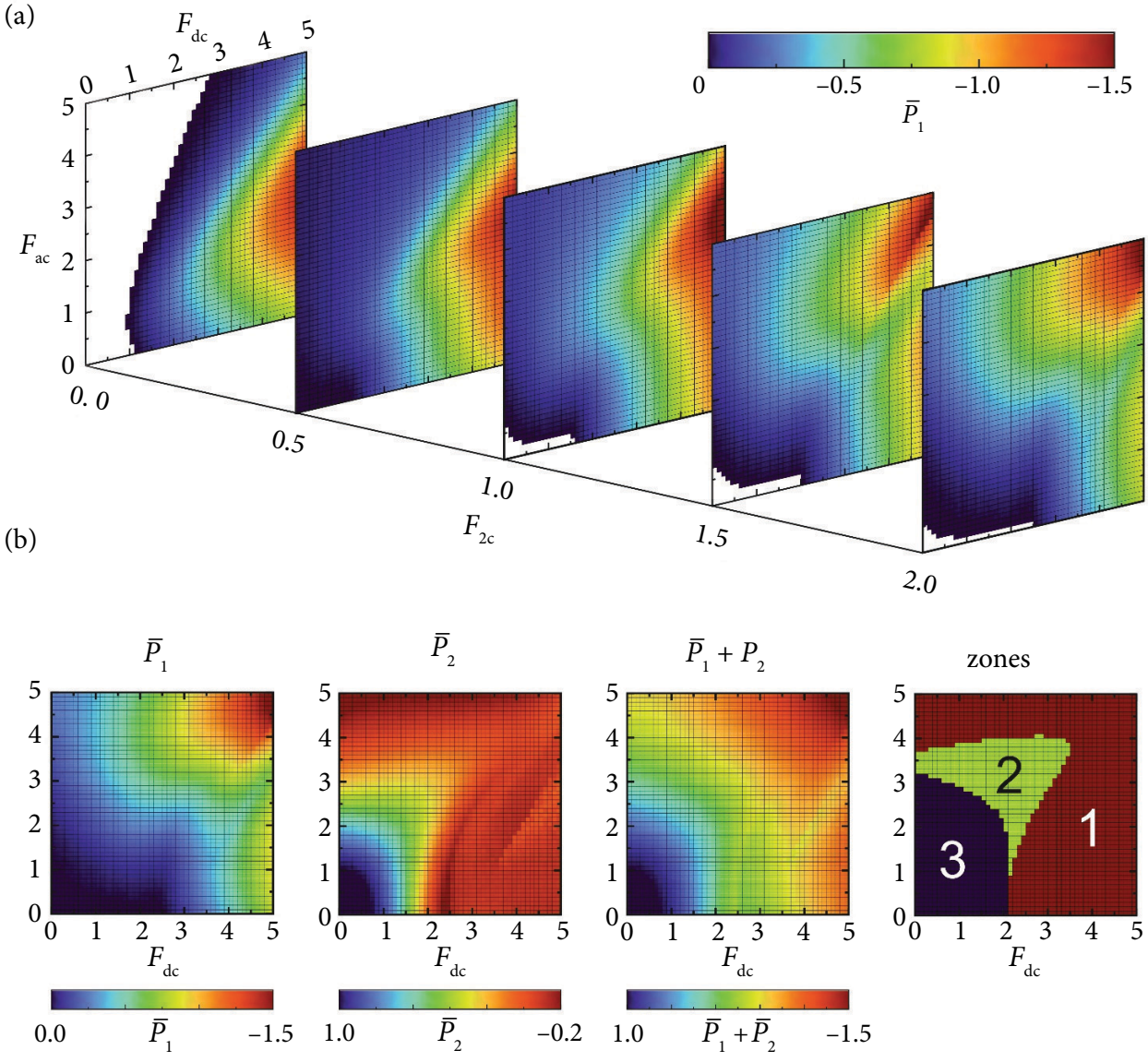

Fig. 3. (a) The maximal probe 1 relative power dependence on biasing conditions and probe 2 electric field strength in the case of 1/2+3/2 non-degenerate gain process. Coloured areas depict the conditions when generation is available, while blank areas depict the conditions when generation is absent. Note the existence of the enlarged generation area compared to that of the non-degenerate process. (b) The leftmost graph corresponds to the maximal probe 1 relative power for the case of $F_2 = 2$, the second left graph depicts the probe 2 relative power corresponding to the probe 1 maximal power conditions. Note the existence of the positive area affecting the total power of the system. The third graph from the left depicts the total relative power $(\bar{P}_1 + \bar{P}_2)$ dependence on biasing conditions. Note the effect of both probe electric fields resulting in different zones, representing possible energy exchange (the rightmost graph) not only between the probe and the pump, but also between the two probes. Further discussion and explanation are given in the text.

(absorption). Obviously, this reflects the total power of the system ($\bar{P} = \bar{P}_1 + \bar{P}_2$), displaying absorbative or generative features. Thus, three zones can be clearly distinguished as depicted on the rightest graph of Fig. 3(b). Zone 1 corresponds to the biasing conditions where the power of both probes is negative:

$$\bar{P}_1 < 0, \quad \bar{P}_2 < 0. \tag{4}$$

Thus, generation on both frequencies is expected. Under such conditions at the current stage of research, it is impossible to tell whether there is an energy exchange between the electric fields of the two probes. On the other hand, zone 2 depicts

the situation wherein the relative power of probe 1 is negative (generative) and the power of probe 2 is positive and smaller by magnitude:

$$\bar{P}_1 < 0, \bar{P}_2 > 0, \quad |\bar{P}_1| > |\bar{P}_2|. \tag{5}$$

In this case, it is quite obvious that the power emitted by probe 1 exceeds the power absorbed by probe 2, therefore, one can claim that the power for probe 1 is supplied as by pump field as by probe 2 field. In zone 3, representing

$$\bar{P}_1 < 0, \bar{P}_2 > 0, \quad |\bar{P}_1| < |\bar{P}_2| \tag{6}$$

conditions, probe 1 emits less power than probe 2 absorbs, hence, the total power is positive. This allows one to make an assumption that all the power required for the probe 1 generation can be supplied by probe 2 solely. These considerations reveal the influence of probe 2 for the generation processes, allowing one to achieve generation at the pump conditions unavailable for the case of degenerate process.

4. Conclusions

Non-degenerate gain processes in biased semiconductor superlattices were analyzed. The large signal gain model was successfully adapted to study the conditions when the generated electric field strength can reach levels comparable to the bias electric field strengths. Analyzing the differences between the degenerate and non-degenerate processes we managed to show that in the case of the latter, the pure parametric generation of fractional harmonics becomes available. It was shown that the transition of the dominating gain mechanism from the Bloch to the parametric one with an increase of F_{ac} remains in the case of non-degenerate gain process and even becomes more distinct. Finally, we revealed that in the case of two probe frequencies participating in the process, the energy can be transferred not only from the bias, but also between the probes. This means that for particular bias conditions, one may expect energy flow from one probe to another. To summarize, the expanded understanding on the processes occurring during the high-frequency generation/amplification paves the basis to develop application-ready generators and/or amplifiers in the THz and sub-THz frequency range.

References

[1] L. Esaki and R. Tsu, Superlattice and negative differential conductivity in semiconductors, IBM J. Res. Dev. **14**(1), 61–65 (1970).

[2] J. Feldmann, K. Leo, J. Shah, D.A.B. Miller, J.E. Cunningham, T. Meier, G. von Plessen, A. Schulze, P. Thomas, and S. Schmitt-Rink, Optical investigation of Bloch oscillations in a semiconductor superlattice, Phys. Rev. B **46**, 7252 (1992).

[3] V.G. Lyssenko, G. Valušis, F. Löser, T. Hasche, K. Leo, M.M. Dignam, and K. Köhler, Direct measurement of the spatial displacement of Bloch-oscillating electrons in semiconductor superlattices, Phys. Rev. Lett. **79**, 301 (1997).

[4] R. Terazzi, T. Gresch, M. Giovannini, N. Hoyler, N. Sekine, and J. Faist, Bloch gain in quantum cascade lasers, Nat. Phys. **3**, 329–333 (2007).

[5] K.F. Renk, B.I. Stahl, A. Rogl, T. Janzen, D.G. Pavel'ev, Yu.I. Koshurinov, V. Ustinov, and A. Zhukov, Subterahertz superlattice parametric oscillator, Phys. Rev. Lett. **95**, 126801 (2005).

[6] K.F. Renk, A. Rogl, and B.I. Stahl, Semiconductor-superlattice parametric oscillator for generation of sub-terahertz and terahertz waves, J. Lumin. **125**(1), 252–258 (2007).

[7] Yu.A. Romanov and Yu.Yu. Romanova, Self-oscillations in semiconductor superlattices, J. Exp. Theor. Phys. **91**, 1033–1045 (2000).

[8] T. Hyart, A.V. Shorokhov, and K.N. Alekseev, Theory of parametric amplification in superlattices, Phys. Rev. Lett. **98**, 220404 (2007).

[9] T. Hyart and K.N. Alekseev, Nondegenerate parametric amplification in superlattices and the limits of strong and weak dissipation, Int. J. Mod. Phys. B **23**, 4403–4413 (2009).

[10] T. Hyart, K.N. Alekseev, and E.V. Thuneberg, Bloch gain in dc-ac-driven semiconductor superlattices in the absence of electric domains, Phys. Rev. B **77**, 165330 (2008).

[11] T. Hyart, N.V. Alexeeva, A. Leppänen, and K.N. Alekseev, Terahertz parametric gain in semiconductor superlattices in the absence of electric domains, Appl. Phys. Lett. **89**(13), 132105 (2006).

[12] Y.A. Romanov, J.Yu. Romanova, L.G. Mourokh, and N.J.M. Horing, Nonlinear terahertz

oscillations in a semiconductor superlattice, J. Appl. Phys. **89**(7), 3835–3840 (2001).

[13] G. Valušis, A. Lisauskas, H. Yuan, W. Knap, and H.G. Roskos, Roadmap of terahertz imaging 2021, Sensors **21**(12), 4092 (2021).

[14] A. Leitenstorfer, A.S. Moskalenko, T. Kampfrath, J. Kono, E. Castro-Camus, K. Peng, N. Qureshi, D. Turchinovich, K. Tanaka, A. Markelz, et al., The 2023 terahertz science and technology roadmap, J. Phys. D **56**, 223001 (2023).

[15] V. Čižas, L. Subačius, N.V. Alexeeva, D. Seliuta, T. Hyart, K. Köhler, K.N. Alekseev, and G. Valušis, Dissipative parametric gain in a GaAs/AlGaAs superlattice, Phys. Rev. Lett. **128**, 236802 (2022).

[16] V. Čižas, N. Alexeeva, K.N. Alekseev, and G. Valušis, Coexistence of Bloch and parametric mechanisms of high-frequency gain in doped superlattices, Nanomaterials **13**(13), 1993 (2023).

[17] G. Haddad and R. Trew, Microwave solid-state active devices, IEEE Trans. Microw. Theory Techn. **50**(3), 760–779 (2002).

[18] J.M. Manley and H.E. Rowe, Some general properties of nonlinear elements – Part I. General energy relations, Proc. IRE **44**, 904 (1956).

SUMINIO DAŽNIO GENERAVIMO IR STIPRINIMO PROCESAI PUSLAIDININKINĖSE SUPERGARDELĖSE

V. Čižas [a], N. Alexeeva [a], K. Alekseev [a], G. Valušis [a, b]

[a] *Fizinių ir technologijos mokslų centro Optoelektronikos skyrius, Vilnius, Lietuva*

[b] *Vilniaus universiteto Fizikos fakulteto Fotonikos ir nanotechnologijų institutas, Vilnius, Lietuva*

Santrauka

Puslaidininkinės supergardelės dėl ypatingos struktūros ir elektronų pernašos pasižymi retais fizikiniais efektais, kurie leidžia kurti skirtingiausius prietaisus, veikiančius terahercų (THz) dažnių ruože. Šiame darbe tiriamos puslaidininkinių supergardelių aukštadažnio signalo stiprinimo galimybės neišsigimusiojo proceso metu. Skirtingai nuo ankstesnių darbų, kai tyrimui buvo naudotas mažo signalo modelis, šiame darbe buvo panaudotas didelio signalo stiprinimo modelis, kuris taikomas atvejams, kai generuojamo signalo elektrinio lauko stipris yra palyginamas su priešįtampio signalu. Gauti rezultatai palyginti su anksčiau atliktais išsigimusiųjų procesų skaičiavimais. Parodyta, kad neišsigimusiojo proceso atveju galimas parametrinis trupmeninių harmonikų generavimas. Taip pat parodyta, kad išsigimusiajam procesui būdingas dominuojančio generavimo mechanizmo perėjimas iš Blocho stiprinimo į parametrinį ne tik išlieka ir neišsigimusiojo proceso atveju, bet ir sustiprėja. Galiausiai parodytas energijos pertekėjimas tarp dviejų neišsigimusiajame procese dalyvaujančių skirtingo dažnio elektrinių laukų. Gauti rezultatai, tikėtina, leis geriau suprasti supergardelėje vykstančius generavimo ir (ar) stiprinimo procesus, leisiančius sukurti mažą, našų, ir galingą THz dažnių ruožo šaltinį ar stiprintuvą.